

DOI: 10.54503/0571-7132-2025.68.1-47

## SPECTRAL VARIATIONS AND PHYSICAL CONDITIONS OF BY DRACONIS IN THE ULTRAVIOLET

M.R.SANAD

Received 17 October 2024

Accepted 14 February 2025

We present International Ultraviolet Explorer (IUE) observations during the period (1980 - 1994) of the double lined spectroscopic binary BY Dra to show the spectral behavior and physical conditions in its atmosphere. The observations reveal indication of flare activity in their flux values in years (1981-1990-1994) in the chromosphere and transition region of the primary star. Beside the flaring activity the emission lines show a range of variations between high, intermediate and low. There is a relation between the fluxes and rotational phase. The reddening of BY Dra was estimated from 2200 Å absorption feature to be  $E(B - V) = 0$ . The average mass loss rate is found to be  $\sim 4.9 \cdot 10^{-8} M_{\odot} \text{ yr}^{-1}$ , the average temperature of the emitting region to be  $\sim 9.2 \cdot 10^4 \text{ K}$ , energy of flare to be  $\sim 6.2 \cdot 10^{37} \text{ erg}$ . We attributed the spectral variations to a cyclic behavior of the underlying magnetic field and the flaring activity to three component model.

*Keywords: stars: activity - stars: flare - stars: magnetic field - Individual: BY Dra - ultraviolet*

1. *Introduction.* BY Dra is a double - lined spectroscopic binary [1] with rotational period of 3.8 days and consists of dk5e + dk7e with an inclination of 30 degrees. The primary star makes up to two thirds of the light from the system at visual wavelengths [2]. BY Dra exhibits a significant brightness asymmetry in spectroscopic studies [3,4].

International Ultraviolet Explorer (IUE) observations have been used to determine the physical conditions in the transition region of flare stars [5]. Rotational variation studies [6] and Doppler imaging of ultraviolet emission lines [7] provide indication of discrete active areas in the chromosphere and transition regions of flare systems.

Stellar magnetic activity is a result of interplay of rotation and turbulent convection at stellar surface. Stellar rotation plays significant role in the dynamo efficiency and influence the magnetic activity of star. Magnetic activity is related to modulations in the stellar magnetic field and consequently is connected to the structure of the stellar subsurface zone, stellar rotation, spectral variations and regeneration of the magnetic field through self - sustaining dynamo activity [8-11].

Helminiak et al. [12] calculated the spectroscopic & astrometric orbital solution and the archival astrometric measurements from the Palomar Testbed Interferometer (PTI) and derived  $M_1 = 0.79 M_\odot$ ,  $M_2 = 0.69 M_\odot$ ,  $d = 16.5$  pc. Vogt & Fekel [3] estimated the radius of the primary star to be  $R_1 = 1.2 R_\odot$ .

Butler et al. [13] by using IUE observations detected a small rotational modulation of the strong ultraviolet emission lines and interpreted this as evidence for plage - type regions in the stellar chromosphere which overlie the photospheric spots and the active regions were so numerous that some were always in view.

In this paper we studied the spectral behaviour of BY Dra binary system by using ultraviolet observations obtained with the IUE. The important observational evidences in our study are that firstly there is a relation between fluxes of emission lines in the times of (high, intermediate & low states) with rotational phase secondly the similar flaring activity at the same phases indicating a possible common origin in the chromosphere and transition region of BY Dra system.

The paper is organized as follows: In section 2 we present the ultraviolet observations, in section 3 we demonstrate the method of reddening determination, section 4 shows the results and discussions of the spectral behaviour of emission lines in the emitting areas, and section 5 contains the conclusions.

*2. Observations and data reduction.* The short wavelength ultraviolet spectra obtained with IUE with low-resolution have been retrieved from the MAST IUE system through its principle center at <https://archive.stsci.edu/iue/>. A detailed description of the ultraviolet data is given by [14,15].

The ultraviolet data were processed by using the standard software of IUEDAC IDL for the processing of spectra. The spectra were referenced to the rotational phase of the BY Dra binary system by using the ephemeris of Rodono et al. [16].

$$\text{HJD} = 2438983.612 + 3^d.836 \cdot E.$$

Table 1 list the ultraviolet observations of BY Dra with low resolution. The spectra were inspected individually in the 1150-1950 Å region to identify and reject noisy and overexposed or underexposed data.

The ultraviolet observations of BY Dra covering most phases. Representative examples of spectral lines are given in Fig.1, showing the variations of line fluxes at different times and the flaring activity. The emission lines are originated in the chromosphere and transition region of BY Dra primary star. Ultraviolet emission lines with different ionizations up to NV 1240 Å, SiIV 1400 Å, and CIV 1550 Å have been found in BY Dra.

### *3. Results and discussions.*

*3.1. Reddening determination of BY Dra.* The method of estimating the reddening of BY Dra depends on using the most suitable set of ultraviolet data

Table 1

## JOURNAL OF IUE OBSERVATIONS OF BY Dra

Data ID	Dispersion	Aperture	H.J.D.	Exposure time (s)	Phase
SWP10354	Low	Large	2444526.09388	7199.819	0.85
SWP15156	Low	Large	2444880.23403	3599.844	0.17
SWP15177	Low	Large	2444882.44178	7199.149	0.75
SWP39725	Low	Large	2448164.18267	5399.627	0.26
SWP39726	Low	Large	2448164.28584	5399.627	0.29
SWP39727	Low	Large	2448164.38215	5819.467	0.31
SWP39733	Low	Large	2448165.17983	5399.627	0.52
SWP39734	Low	Large	2448165.35733	5579.851	0.57
SWP39738	Low	Large	2448166.14191	4499.736	0.77
SWP39739	Low	Large	2448166.23425	4499.736	0.80
SWP39740	Low	Large	2448166.32384	3599.844	0.82
SWP39746	Low	Large	2448167.29306	4499.736	0.06
SWP39747	Low	Large	2448167.33983	2339.505	0.08
SWP39755	Low	Large	2448168.23925	4499.736	0.32
SWP39756	Low	Large	2448168.33443	2699.544	0.34
SWP39761	Low	Large	2448169.07016	1799.652	0.54
SWP42778	Low	Large	2448551.09764	22199.77	0.13
SWP48664	Low	Large	2449248.23067	4499.736	0.86
SWP50631	Low	Large	2449469.43293	7198.609	0.53
SWP51395	Low	Large	2449544.73564	7199.819	0.16

of Short Wavelength Prime camera (SWP) with low resolution ( $6 \text{ \AA}$ ) in the wavelength range of between  $1150\text{-}1950 \text{ \AA}$  and Long Wavelength Redundant (LWR) camera with low resolution ( $6 \text{ \AA}$ ) in the wavelength range between  $2000\text{-}3000 \text{ \AA}$ . The Short Wavelength ultraviolet spectra are binned in  $15 \text{ \AA}$  bins and  $25 \text{ \AA}$  bins for Long Wavelength spectra. The collection of short and long wavelength data gives the ultraviolet spectrum shape of a reddened star, with its characteristic depression at  $2200 \text{ \AA}$ . The following ultraviolet observations are used in estimating the value of reddening (SWP10354 - LWR09021) (SWP15177 - LWR11687) (SWP39740 - LWR18894) leading to the best smoothing spectrum suitable for determining the reddening value.

The most suitable value is determined by visual examination of the plots for the best fit to the  $2200 \text{ \AA}$  absorption feature, which represented the best agreement between observations and standard theoretical (dashed line) values. The estimated value of the reddening for BY Dra is  $E(B - V) = 0.00$  as shown in Fig.2.

3.2. *Spectral variations and its source.* BY Dra binary system show some ultraviolet emission lines observed with IUE SWP camera for chromospheric cooler area such as CI  $1657 \text{ \AA}$ , OI  $1306 \text{ \AA}$ , SII  $1808 \text{ \AA}$  and for transition hotter

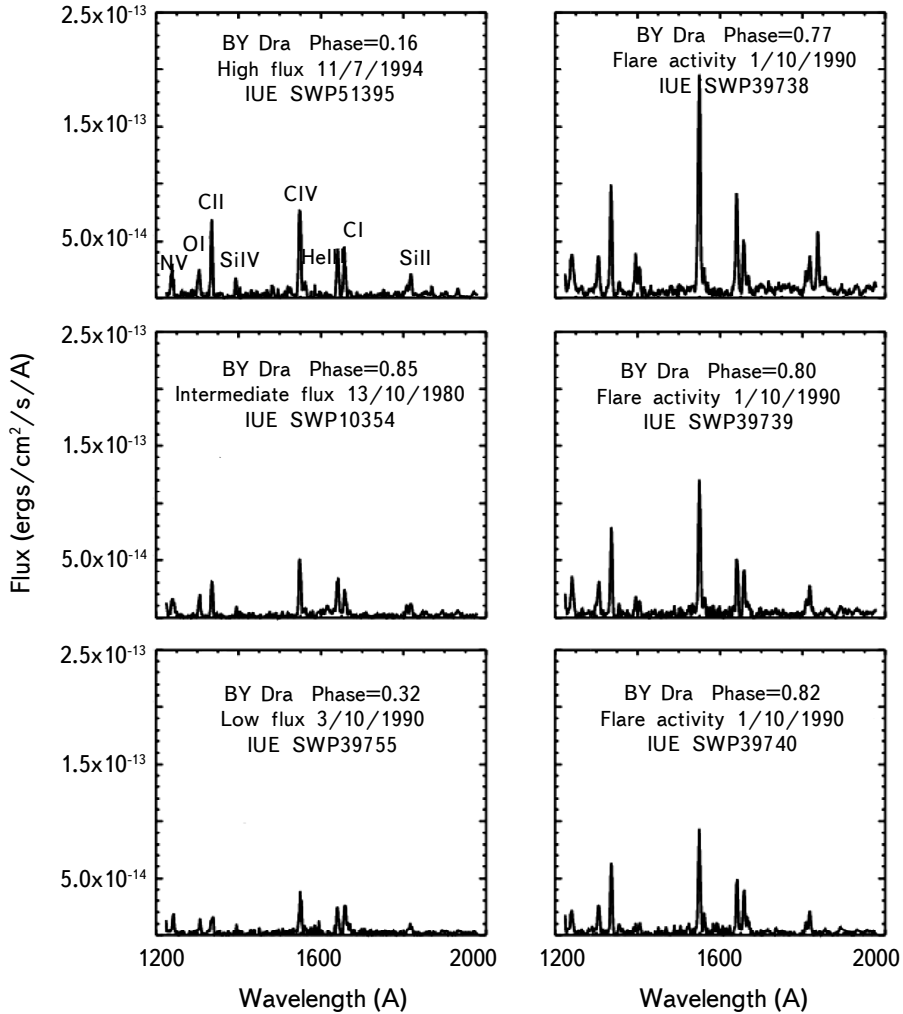


Fig.1. IUE spectrum of BY Dra with high, intermediate and low flux at different phases at the left - hand side and the flaring activity at the right - hand side.

area such as CII 1335 Å , SIV 1400 Å , CIV 1550 Å , HeII 1640 Å , NV 1240 Å , and SiIII 1892 Å [13].

The OI, SiIV, CIV, CI, CII are resonance emission lines that are collisionally excited by the physical conditions of plasma in the quiet chromosphere. The HeII emission line is a recombination line. These emission lines are produced in the chromosphere and transition region of the primary star.

The emission lines (OI, CI) with low variable fluxes have nearly the same spectral behavior indicating that they have the same emitting region, the chromosphere of the primary star, while the emission lines (CII, CIV, HeII) with flaring

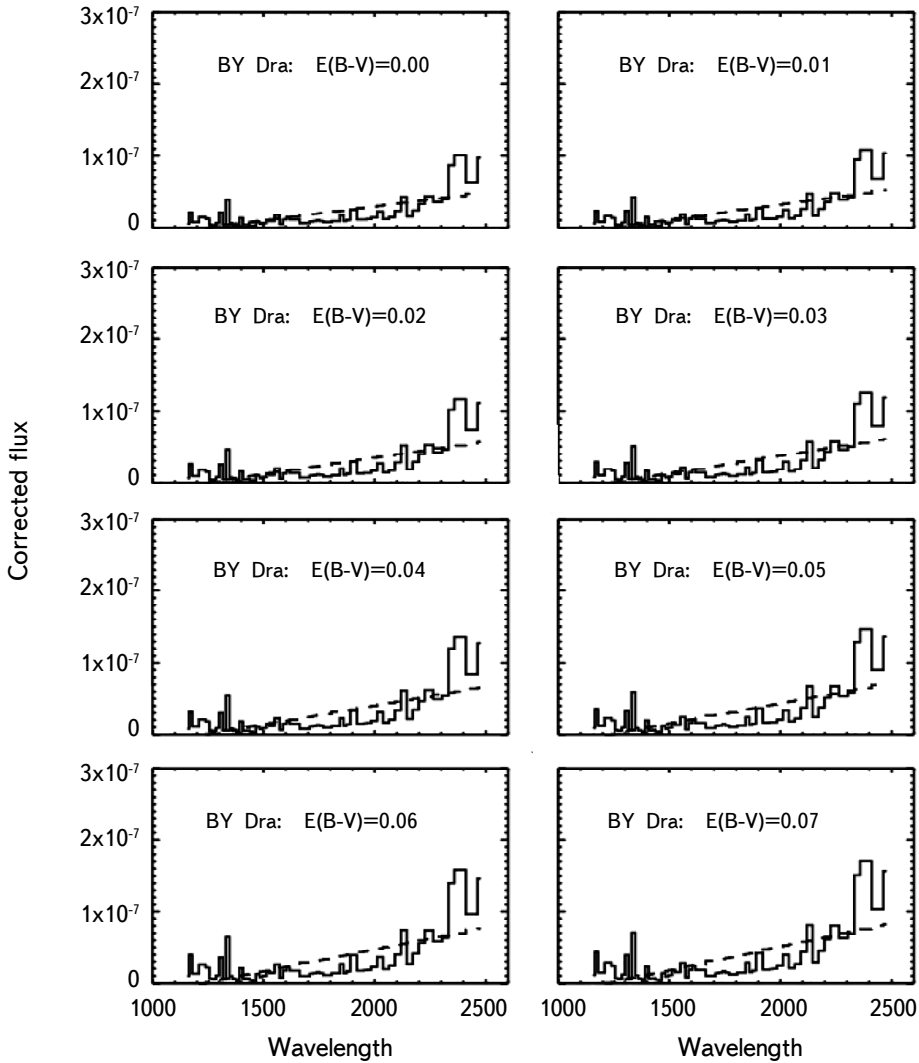


Fig.2. Reddening determination of BY Dra binary system.

activity indicating that they have the same emitting region, transition region of the primary star. The fluxes in emission lines were measured by determining the integrated area included in the emission area above the continuum near the wings of spectral line and were calculated with the method of Gaussian profile fitting.

Fig.3 shows the fluxes of chromospheric and transition region emission lines with rotational phase. The line fluxes correlate and change with phase with different values on short timescales of some hours and long timescales of months and years for the period 1980-1994. The line fluxes of both chromospheric region

(OI & CI) and transition region (NV, CII, CIV, He II) change between high, intermediate and low values with symbol (+) while the symbol ( $\diamond$ ) represents flaring activity.

Tables 2-7 reveal the fluxes and values of flare of selected emission lines for BY Dra. The flaring activity of BY Dra for ultraviolet observations is not periodic as II Peg and  $\lambda$  And binary systems [17-19]. The increase in flux of emission lines reached about four times the quiescent values and the activity of emission lines is around phases (0.20 and 0.80) as showed in Fig.3.

Butler et al. [13] detected a true modulation of the ultraviolet emission line fluxes. This variation is in the sense that the ultraviolet emission lines are stronger at maximum spot visibility, suggestive of association with plage type areas in the chromosphere and transition region in the vicinity in the cool photospheric spots. The strong SWP emission lines are come from allowed transitions, their emissivities are not greatly affected by density and pressure changes. They deduced that most of the hot material in the atmosphere is contained in magnetic loops [20,21]. So, the increase in the amount of high temperature material relative to the amount of low temperature material could be explained by the presence of extensive magnetic loops in the atmosphere of BY Dra.

De Jager et al. [22] presented a study of simultaneous observations in the visual, radio and X-ray ranges of stellar flares on the BY Dra binary system. They observed one significant flare, simultaneously in soft X-rays and visible wavelengths and one smaller burst. The main flare generated hot plasma emitting soft X-rays. They suggested a model in which the flare starts impulsively by heating the stellar photosphere by particle beams with a temporary hot hole burnt into photosphere.

The relation of emission line fluxes with phase for chromosphere of the primary star of BY Dra can be interpreted as follows: The stellar atmosphere has undergone to magnetic field resulted in its non - radiative heating. The magnetic activity in late type stars is analogous to that observed with the Sun. It is assumed that magnetic fields produced from an interaction between convection currents and differential rotation as contained in the dynamo process. The hot area of plasma is pushed by magnetic fields upward and leaving cool regions as dark spots with low temperature in the outer parts.

The spot activity is explained as a result of a magnetic dynamo affecting on the convective area and the magnetic activity is variable with time. The variation of line fluxes gives an indication of active areas in the chromosphere of the primary star. These active areas are near the spot group with short term variations in the spot arrangement and the variations of ultraviolet emission lines suggesting a hot area overlying a cool spot.

The ultraviolet observations with enhanced emission lines as flaring activity

in the transition region of BY Dra can be understood by the three - component model of Jeffries [23]. In this model the thickness of the transition area is not constant over the surface of star and consists of three regions: active, quiet and cool loops underlying the hot coronal loops characterized by low and high ultraviolet emission occurring in the vicinity of spots required to interpret the low and high temperature components [24].

In this interpretation an area of cooling plasma is produced under a rising

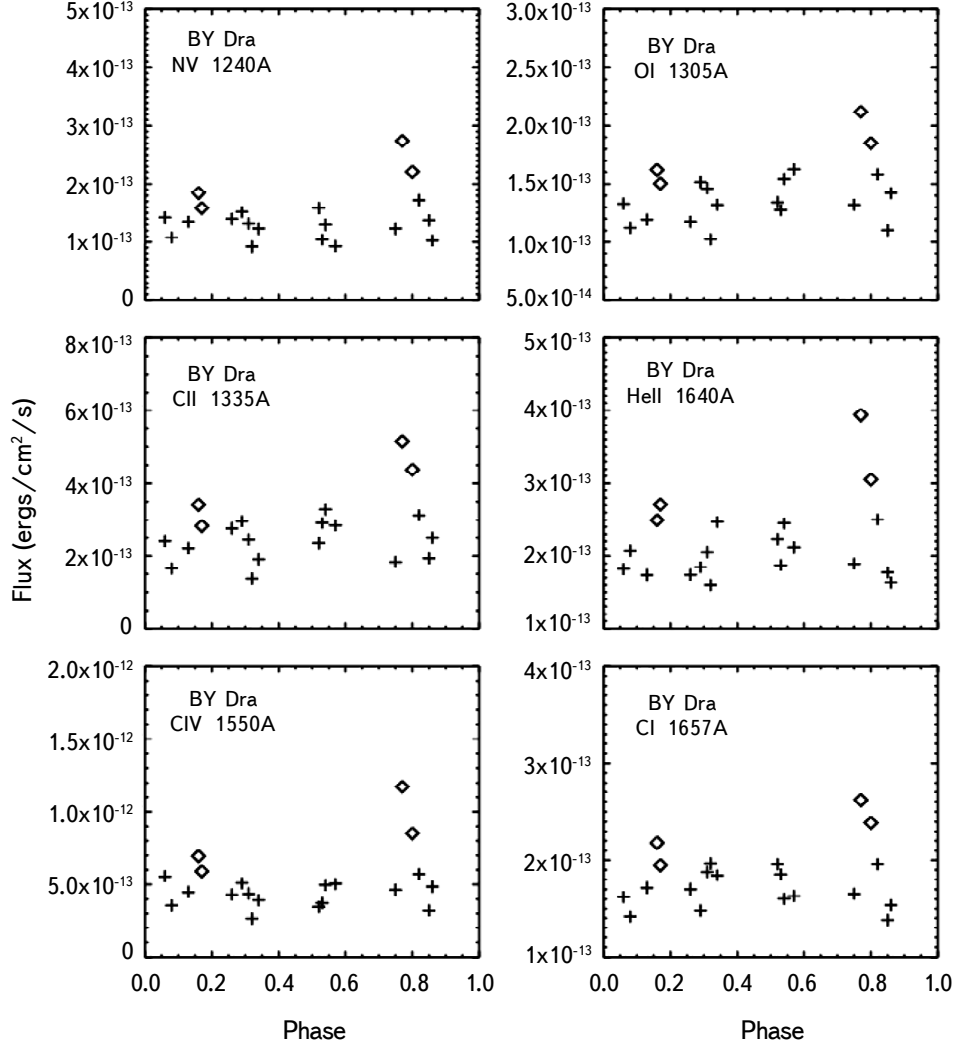


Fig.3. Spectral variations with rotational phase for line fluxes (OI & CI) of chromospheric region and line fluxes (NV, CII, CIV, HeII) of transition region. symbol (+) represents normal spectral variations between high, intermediate and low values while the symbol ( $\diamond$ ) represents flaring activity.

magnetic reconnection line. It is believed that flaring occurs on several scales in the stellar atmosphere. Suggesting that the heating of the corona is achieved by a quasi-continuous flaring process [25].

If this source of activity stopped then the plasma in the loops of active area will cool by radiative means and at some time the plasma will be a source of ultraviolet radiation. So, the energy source is large scale migration of active areas causing loops to interact leading to flare heating of the loop plasma. This physical process for the formation of the cool plasma represents the main mechanism of the flaring activity.

In conclusion, the IUE observations of BY Dra shows presence of hot material through rotation period suggesting that BY Dra has magnetic loops that remain visible for long periods of time and changes by rotation. The fact that the line fluxes remain high suggests that the active regions and loops in addition to spots are either quite long lived on BY Dra or they are numerous that some are always presented by Butler et al. [13].

During the flare process, the electrons are accelerated with high energies and stream down along the flare loop and heating the emitting transition region and generating significant flare emission. The ultraviolet emission with flare energies can be produced either by accelerating the energetic electrons in flare or by impact excitations by high energy electrons as non - thermal excitation or by thermal conduction [26].

4. *Ultraviolet luminosity, flare energy, mass loss rate and temperature of emitting area.* The ultraviolet luminosity of emitting region is calculated by using the following equation

$$L_{UV} = 4\pi Fd^2,$$

where  $F$  is the integrated flux value and  $d$  is the distance to the object 16.5 pc [12]. For BY Dra binary system, by using integrated fluxes of NV, OI, CII, CIV, HeII and CI, it is found that the ultraviolet luminosities for the selected spectral lines in different states as listed in the following Tables 2-7.

By using the mass of the primary star  $M \sim 0.79 M_{\odot}$  [12], and a radius of  $\sim 1.4 R_{\odot}$  [3] the rate of mass loss is calculated by using the following equation [27].

$$\log M^* = 14.02 + 1.24 \log\left(\frac{L}{L_{\odot}}\right) + 0.16 \log\left(\frac{M}{M_{\odot}}\right) + 0.81 \log\left(\frac{R}{R_{\odot}}\right) M_{\odot} \text{ yr}^{-1}.$$

The mass loss rate is estimated to be  $\sim 4.9 \cdot 10^{-8} M_{\odot} \text{ yr}^{-1}$ .

The stored energy in the flare for the G star is estimated by using the following equation, [28]:

$$W_{primary} = 1.6 \cdot 10^{37} \left(\frac{l}{R_{\odot}}\right) \left(\frac{R}{R_{\odot}}\right)^2 \left(\frac{B_{surf}}{1000 G}\right) \text{ erg}.$$



By using the magnetic field strength of 2700 G and  $l = 2R_{\odot}$  [28,29] and a radius of  $\sim 1.4R_{\odot}$ , it is found that the stored energy  $\sim 6.2 \cdot 10^{37}$  erg. Then the temperature of the emitting region is

Table 2

LINE FLUXES AND ULTRAVIOLET LUMINOSITIES AT  
DIFFERENT STATES OF NV

State	Flux ( $\text{erg cm}^{-2} \text{s}^{-1}$ )	$L_{uv}$ ( $\text{erg cm}^{-2} \text{s}^{-1}$ )
Flare	$2.14 \cdot 10^{-13}$	$6.98 \cdot 10^{27}$
High	$1.98 \cdot 10^{-13}$	$5.32 \cdot 10^{27}$
Intermediate	$1.42 \cdot 10^{-13}$	$4.40 \cdot 10^{27}$
Low	$1.02 \cdot 10^{-13}$	$3.31 \cdot 10^{27}$

Table 3

LINE FLUXES AND ULTRAVIOLET LUMINOSITIES AT  
DIFFERENT STATES OF OI

State	Flux ( $\text{erg cm}^{-2} \text{s}^{-1}$ )	$L_{uv}$ ( $\text{erg cm}^{-2} \text{s}^{-1}$ )
Flare	$2.14 \cdot 10^{-13}$	$6.98 \cdot 10^{27}$
High	$1.98 \cdot 10^{-13}$	$5.32 \cdot 10^{27}$
Intermediate	$1.42 \cdot 10^{-13}$	$4.40 \cdot 10^{27}$
Low	$1.02 \cdot 10^{-13}$	$3.31 \cdot 10^{27}$

Table 4

LINE FLUXES AND ULTRAVIOLET LUMINOSITIES AT  
DIFFERENT STATES OF CII

State	Flux ( $\text{erg cm}^{-2} \text{s}^{-1}$ )	$L_{uv}$ ( $\text{erg cm}^{-2} \text{s}^{-1}$ )
Flare	$5.15 \cdot 10^{-13}$	$1.69 \cdot 10^{28}$
High	$4.08 \cdot 10^{-13}$	$1.12 \cdot 10^{28}$
Intermediate	$2.75 \cdot 10^{-13}$	$8.06 \cdot 10^{27}$
Low	$1.37 \cdot 10^{-13}$	$4.50 \cdot 10^{27}$

Table 5

LINE FLUXES AND ULTRAVIOLET LUMINOSITIES AT  
DIFFERENT STATES OF CIV

State	Flux ( $\text{erg cm}^{-2} \text{s}^{-1}$ )	$L_{uv}$ ( $\text{erg cm}^{-2} \text{s}^{-1}$ )
Flare	$1.17 \cdot 10^{-12}$	$3.85 \cdot 10^{28}$
High	$7.28 \cdot 10^{-13}$	$1.74 \cdot 10^{28}$
Intermediate	$5.04 \cdot 10^{-13}$	$1.43 \cdot 10^{28}$
Low	$2.65 \cdot 10^{-13}$	$8.71 \cdot 10^{27}$

Table 6

LINE FLUXES AND ULTRAVIOLET LUMINOSITIES AT  
DIFFERENT STATES OF HeII

State	Flux (erg cm <sup>-2</sup> s <sup>-1</sup> )	$L_{uv}$ (erg cm <sup>-2</sup> s <sup>-1</sup> )
Flare	$4.24 \cdot 10^{-13}$	$1.39 \cdot 10^{28}$
High	$2.71 \cdot 10^{-13}$	$8.91 \cdot 10^{27}$
Intermediate	$2.05 \cdot 10^{-13}$	$6.75 \cdot 10^{27}$
Low	$1.59 \cdot 10^{-13}$	$5.24 \cdot 10^{27}$

Table 7

LINE FLUXES AND ULTRAVIOLET LUMINOSITIES AT  
DIFFERENT STATES OF CI

State	Flux (erg cm <sup>-2</sup> s <sup>-1</sup> )	$L_{uv}$ (erg cm <sup>-2</sup> s <sup>-1</sup> )
Flare	$2.61 \cdot 10^{-13}$	$8.60 \cdot 10^{27}$
High	$2.01 \cdot 10^{-13}$	$6.59 \cdot 10^{27}$
Intermediate	$1.80 \cdot 10^{-13}$	$5.36 \cdot 10^{27}$
Low	$1.38 \cdot 10^{-13}$	$4.54 \cdot 10^{27}$

$$T = 9.2 \cdot 10^4 \text{ K} \pm 500 \text{ K}.$$

5. *Conclusions.* The main two aims of this study are to firstly study the spectral behaviour and flaring activity of transition region and secondly the richness of the observations allowed estimation of some physical parameters of BY Dra binary system by using International Ultraviolet Explorer (IUE) data.

The emission lines of (NV, OI, CI, CII, CIV, HeII) are produced in chromosphere and transition region of the primary star. The emitting regions are characterized by variations of the magnetic activity and the results showed a relation between rotational phase and line fluxes.

The flaring activity of transition region reveals an increase in fluxes of three emission lines (CII, CIV, HeII) reached about four times the quiescent values and the activity of all emission lines is around certain phases.

The estimated physical parameters (ultraviolet luminosity, mass loss rate, stored energy in flare and temperature) support the origin of ultraviolet emission lines in the chromosphere and transition region of the primary star.

The flaring activity support the three - component model in which the thickness of the transition area is not constant over the surface of star and consists of three regions active, quiet and cool loops underlying the hot coronal loops

characterized by low and high ultraviolet emission occurring in the vicinity of spots and the cool material is related to flare activity with an area of cooling plasma produced under a rising magnetic reconnection line. The energy source is large scale migration of active areas causing loops to interact leading to flare heating of the loop plasma.

Astronomy Department, National Research Institute of Astronomy and Geophysics Helwan-Cairo-Egypt, e-mail: mrsanad1@yahoo.com

## СПЕКТРАЛЬНАЯ ПЕРЕМЕННОСТЬ И ФИЗИЧЕСКИЕ УСЛОВИЯ BY Dra В УЛЬТРАФИОЛЕТЕ

М.Р.САНАД

Представлены наблюдения IUE спектрально-двойной звезды BY Dra в период с 1980 по 1994гг., с целью показать спектральное поведение и физические условия в ее атмосфере. Наблюдаемые значения потока в 1981, 1990 и 1994гг. указывают на вспышечную активность первичной звезды в хромосфере и переходной области. Помимо вспышечной активности, наблюдается переменность эмиссионных линий от больших до средних и низких значений. Обнаружена связь между потоками и фазой вращения. Покраснение BY Dra было оценено по поглощению на длине волны  $2200 \text{ \AA}$  как  $E(B - V) = 0$ . Средняя скорость потери массы составляет  $\sim 4.9 \cdot 10^{-8} M_{\odot}$  в год, средняя температура излучающего региона, рассчитанная по уравнению Планка, составляет  $\sim 9.2 \cdot 10^4$  К, энергия вспышки -  $\sim 6.2 \cdot 10^{37}$  эрг. Предположено, что спектральная переменность связана с циклическим поведением магнитного поля, а активность вспышек - с трехкомпонентной моделью.

Ключевые слова: *звезды: активность - звезды: вспышки звезды: магнитное поле - BY Dra - ультрафиолет*

## REFERENCES

1. *W.Krzeminski, R.P.Kraft*, Astron. J., **72**, 307, 1967.
2. *B.R.Pettersen, K.Olah, W.H.Sandmann*, Astron. Astrophys., **96**, 497, 1992.
3. *S.S.Vogt, F.Fekel*, Astrophys. J., **234**, 958, 1979.

4. *P.B.Lucke, M.Mayor*, *Astron. Astrophys.*, **92**, 182, 1980.
5. *M.R.Sanad, I.Zead, M.A.Abdel-Sabour*, *Astrophysics*, **64**, 316, 2021.
6. *N.Marstad*, In: *Advances in Ultraviolet Astronomy, Four Years of IUE Research*, p.554, 1982.
7. *F.M.Walter, J.E.Neff, D.M.Gibson et al.*, *Astron. Astrophys.*, **186**, 241, 1987.
8. *E.N.Parker*, *Astrophys. J.*, **122**, 293, 1955.
9. *A.Skumanich*, *Astrophys. J.*, **171**, 565, 1972.
10. *R. de Grijs, D.Kamath*, *Universe*, **7**, 440, 2021.
11. *D.Chahal, R. de Grijs, D.Kamath et al.*, *Mon. Not. Roy. Astron. Soc.*, **514**, 4932, 2022.
12. *K.G.Helminiak, M.Konacki, M.W.Muterrspaugh*, *Mon. Not. Roy. Astron. Soc.*, **419**, 1285, 2012.
13. *C.J.Butler, J.G.Doyle, A.D.Andrews et al.*, *Astron. Astrophys.*, **174**, 139, 1987.
14. *P.M.Rodriguez-Pascual, R.Gonzalez-Riestra, N.Schartel et al.*, *Astron. Astrophys.*, **139**, 183R, 1999.
15. *R.Gonzalez-Riestra, A.Cassatella, W.Wamsteker*, *Astron. Astrophys.*, **373**, 730G, 2001.
16. *M.Rodono, G.Cutispoto, V.Pazzani et al.*, *Astron. Astrophys.*, **165**, 135, 1986.
17. *M.R.Sanad*, *Research in Astron. Astrophys.*, **22**(8), 085015, 2022.
18. *M.R.Sanad*, *Astron. Rep.*, **67**, 581, 2023.
19. *M.R.Sanad*, *Astron. Astrophys. Transactions*, **34**, 163, 2024.
20. *G.I.Withbroe*, *Astrophys. J.*, **225**, 641, 1987.
21. *J.G.Doyle, J.C.Raymond*, *Solar phys.*, **90**, 97, 1984.
22. *C. De Jager, J.Heise, S.Avgoloupis et al.*, *Astron. Astrophys.*, **156**, 95, 1986.
23. *R.D.Jeffries*, *Mon. Not. Roy. Astron. Soc.*, **253**, 369, 1991.
24. *J.C.Raymond, R.Foukal*, *Astrophys. J.*, **253**, 323, 1982.
25. *E.N.Parker*, *Astrophys. J.*, **330**, 474, 1988.
26. *T.G.Forbes, E.R.Priest*, *Astrophys. J.*, **446**, 377, 1995.
27. *H.Nieuwenhuizen, C. de Jager*, *Astron. Astrophys.*, **231**, 134, 1990.
28. *G.H.J. Van den Oord*, *Astron. Astrophys.*, **205**, 167, 1988.
29. *D.O.Fionnagain, A.A.Vidotto, P.Petit et al.*, *Mon. Not. Roy. Astron. Soc.*, **500**, 3438, 2021.